Journal of Hydrology 574 (2019) 660–671

Contents lists available at ScienceDirect

Journal of Hydrology

journal homepage: www.elsevier.com/locate/jhydrol

Research papers

River basin-scale flood hazard assessment using a modified multi-criteria decision analysis approach: A case study

Amirhossein Shadmehri Toosi[a], Giancarlo Humberto Calbimonte[b], Hamideh Nouri[c,d], Sina Alaghmand[e,*]

[a] Department of Civil Engineering, Ferdowsi University of Mashhad, Mashhad, Khorasan Razavi, Iran
[b] Department of Civil & Architectural Engineering and Mechanics, The University of Arizona, Tucson, AZ, USA
[c] Faculty of Engineering Technology, University of Twente, 7500 AE Enschede, The Netherlands
[d] Division of Agronomy, University of Göttingen, Von-Siebold-Strasse 8, 37075 Göttingen, Germany
[e] Department of Civil Engineering, Monash University, 23 College Walk, Clayton, VIC 3800, Australia

ARTICLE INFO

This manuscript was handled by G. Syme, Editor-in-Chief, with the assistance of Ji Chen, Associate Editor

Keywords:
River basin management
Flood hazard mapping
SWAT
Analytical hierarchy process
GIS application

ABSTRACT

Flood is a major natural hazard with extremely large impact on social-ecological systems. Therefore, developing reliable and efficient tools to identify areas vulnerable to potential flooding is vital for water managers, engineers and decision makers. Moreover, being able to accurately classify the level of hazard is a step forward towards more efficient flood hazard mapping. This study presents a multi-criteria index approach to classify potential flood hazards at the river basin scale. The presented methodology was implemented in the Mashhad Plain basin in North-east Iran, where flood has been a major issue in the last few decades. In the present study, seven factors, selected based on their greater influence towards flooding, were identified and extracted from the basic thematic layers to be used to generate a five-class Flood Hazard Index (FHI) map. The Soil and Water Assessment Tool (SWAT) was used to develop a runoff coefficient map, which was found to be the most influential factor. A sensitivity analysis was performed and the results incorporated to generate a modified Flood Hazard Index (mFHI) map. The accuracy of the proposed method was evaluated against the well-documented flood records in the last 42 years at the study area. The results showed that, for both FHI and mFHI maps, more than 97% of historical flood events have occurred in moderate to very high flood hazard areas. This demonstrates that incorporating hydrological model (such as SWAT) and multi-criteria analysis introduces a robust methodology to generate comprehensive potential flood hazard maps. Moreover, the proposed modified methodology can be used to identify high potential flood hazard zones and work towards more efficient flood management and mitigation strategies.

1. Introduction

Natural disasters caused by hydro-meteorological events (including droughts, floods, storms, wildfires, and temperature extremes) are by far the most frequent in the world, and result in the major cause of loss, representing a significant portion of the worldwide disaster loss burden (CRED, 2009; Kourgialas and Karatzas, 2011; Kowalzig, 2008; Luber and Lemery, 2015; McMichael, 2003). From 1900 to 2013, floods and storms associated with high precipitation events accounted for 87% of extreme weather disasters, while, landslides, droughts, extreme temperatures, wildfires and heat accounted for the remainder (CRED, 2009). Accelerated climate change has been recorded in recent decades, which is of particular concern as it may lead to more frequent and severe rainfall events around the world in the future, particularly in arid and semi-arid areas (CRED, 2009; Kain et al., 2018). In order to assess this natural phenomenon, it is required to quantify the consequences of flooding more comprehensively depending on the characteristics of the region including population density, land use, geophysical and climatic factors (Maggioni and Massari, 2018).

Over the past twenty years, space agencies have agreed to reinforce flood monitoring from space, due to the potential growth of remote sensing (RS) application techniques to monitor floods, and its use to address limitations of field data availability (Grimaldi et al., 2016; Grimaldi et al., 2018; Khorrami et al., 2019; Li et al., 2018; Li et al., 2016; Wright et al., 2018). Many studies have been conducted to identify the main factors contributing to the severity of floods

* Corresponding author.
E-mail address: sina.alaghmand@monash.edu (S. Alaghmand).

https://doi.org/10.1016/j.jhydrol.2019.04.072
Received 28 December 2018; Received in revised form 20 March 2019; Accepted 23 April 2019
Available online 24 April 2019

(Alaghmand et al., 2010; Kourgialas and Karatzas, 2017a; Udin et al., 2018; Woldesenbet et al., 2018; Xiao et al., 2017; Zhao et al., 2018). A variety of methods can be used to incorporate different criteria into an integrated tool for both flood prediction and mitigation, depending on the availability of data (Anand et al., 2018; Bradford and Denich, 2007; Dao et al., 2009; Jajarmizadeh et al., 2016; Morris et al., 2010; Neale and Weir, 2015; Tehrany et al., 2013). In this regard, the Multi Criteria Decision Analysis (MCDA) technique has been widely used for integrating, identifying or rating controlling factors, particularly in natural hazard and suitability analysis (Al-shabeeb, 2016; Chowdhury et al., 2010; Jozaghi et al., 2018; Kourgialas and Karatzas, 2017a; Nefeslioglu et al., 2013; Sinha et al., 2008).

Udin et al. (2018) in a case study in the southern district of Kuala Krai, Kelantan, Malaysia, investigated the region exposed to floods through questionnaires and regional data gathering, and categorized the flood zones by using GIS and it was established that parameters such as flood depth, water level, and the amount of rainfall had a major influence on the river flood hazard maps pattern. Kourgialas and Karatzas (2016) estimated flood hazard in the Mediterranean island of Crete in Greece, selecting several contributing factors combined through GIS environment to identify the areas most at risk of flooding under current and future climate conditions. In order to test the reliability of the output flood hazard map, historical flood records were used. Kazakis et al. (2015b) presented an alternative of a multi-criteria index calculation process in order to provide an assessment of flood risk at a regional scale by using spatial analyses. To test the method for accuracy, the index calculation was subject to a sensitivity analysis, including a range of weight values for different scenarios. The analysis showed a good correlation between historical flood event records and the output index data, proving the validity of the results. Chen et al. (2015) in a case study in the Bowen Basin in Queensland, Australia developed a methodology for decision makers to use a spatial multi criteria prototype for evaluation of flood risk at a regional scale using spatial gridded data including topography, land cover and soils type information, hydrology and climate data. According to the indices derived from time series of observations and spatial modeling, a regional flooding risk map was used to illustrate possible impacts of each of the selected criterion indices related to flood analysis towards the level of risk obtained. The maximum flood extent perceivable by time series of RS imagery was used to verify derived map.

Flood hazard mapping represents a great challenge due to the subjectivity of the flood related criterion indices assumed for a basin, and the proper selection of the most sensitive parameters in a basin model. The validation of a flood hazard map may become a challenging process given the fact that the data may not attempt to describe the likelihood of a single real event, but rather an attempt to describe areas affected by all events of a certain magnitude, especially in the case of global flood models at coarse resolutions (Sampson et al., 2015). There is a high demand of emergency services and local institutions for risk based forecasts in terms of flood-prone areas, which require forcing the global flood models to include large and small scale analysis (Dottori et al., 2016). The challenges due to lack of available data over ungagged rural areas, and a rather simple tool to model all the flood related parameters in a basin may also represent an obstacle for an accurate and practical flood hazard assessment at a basin scale. A combination of the techniques mentioned previously in the works cited was used in the present study, but also including other factors to be considered such as runoff coefficient as a flood hazard criterion, as well and GIS computer-based software tools to develop a rainfall runoff response based on high quality terrain data.

Instead of assessing flood hazards through MCDA applied directly to spatial parameters of the basin, the present methodology utilizes different tools and techniques to identify, rank, and validate the flood hazard assessment of a basin unit, not only using its geophysical parameters, but also based on the simulation of its rainfall-runoff response.

Flood hazard assessment is highly regional specific due to spatial and temporal variability of the dominant drivers (e.g. climate, hydrology, topography, agronomy and soil). A sensitivity analysis was also performed to reduce the level of uncertainty due to the subjectivity of parameters commonly selected using judgement by expertise, as well as the uncertainty due to the availability and size of the sample data.

In general, flooding is heavily influenced by naturally high rainfall variability in Iran (Modarres and Sarhadi, 2009; Tabari et al., 2012). This paper describes the integrated application of GIS and multiple-criteria decision analysis (MDCA) techniques coupled with Soil and Water Assessment Tool (SWAT) (Gassman et al., 2010), over the study area denominated Mashhad Plain Basin (MPB), located in Mashhad, Iran. In this modified approach, in addition to the thematic layers, runoff coefficient maps derived from SWAT model have also been included. The present study aimed to: (1) introduce a flood hazard index based on hydrological modeling to identify flood-prone areas in data scarce regions, (2) develop a sensitivity analysis of each of the criteria selected, and compare FHI and mFHI map results with the last 42 years recorded events to validate the accuracy of the proposed approach.

2. Methods and materials

The proposed methodology is an innovative combination of techniques and use of data to identify flood prone areas. The proposed method includes some successive steps which are presented briefly in Fig. 1.

2.1. Study area

The methodology was applied to Mashhad Plain Basin (MPB) located in the northeast of Iran with an area of 9,762 (km^2), between 35° 59′ N to 37° 03′ N latitude and 60° 06 to 58° 22′ E longitude (Fig. 2). The study area has semi-arid to arid climate, with an average monthly temperature ranging from 11.6 °C to 26.7 °C. The annual average precipitation is 262 (mm), ranging from 178 to 381 mm (IRIMO, 2016). There are 28 rain gauge stations available with 24 years of well-documented data (1991–2015). The average land slope is 16.2% and the mean elevation of the basin is 1487 m Above Sea Level (ASL) with minimum and maximum elevation of 856 and 3247 m ASL, respectively.

2.2. Available data

The available data from various governmental organizations and other direct sources such as field surveys and RS data (satellite images) were acquired, as listed in Table 1. Data processing and analysis is detailed in Sections 2.3–2.5.

2.3. Flood hazard index (FHI)

In this study, seven criteria as listed in Table 2 were identified to determine FHI. The selection of these criteria was based on their proven effectiveness, as documented in the literature review (Dottori et al., 2016; Kourgialas and Karatzas, 2016; Kourgialas and Karatzas, 2017a; Xiao et al., 2017; Zhao et al., 2018). In addition to the selected criteria parameters used for the FHI calculation, expressed in thematic layers, a hydrological model (SWAT) was used through GIS tools to estimate the necessary spatial hydrological parameters and to determine the site attributes associated with the selected criteria (Alaghmand et al., 2012a; Alaghmand et al., 2012b). To delineate flood potential zones, all the thematic layers along with their normalized weights were integrated using ArcGIS software. Using the Weighted Linear Combination (WLC), total normalized weights of different features were overlaid in the integrated raster layer as follows:

$$FHI = \sum x_i w_i = R_i w_i + E_i w_i + S_i w_i + D_i w_i + RI_i w_i + ER_i w_i + L_i w_i \quad (1)$$

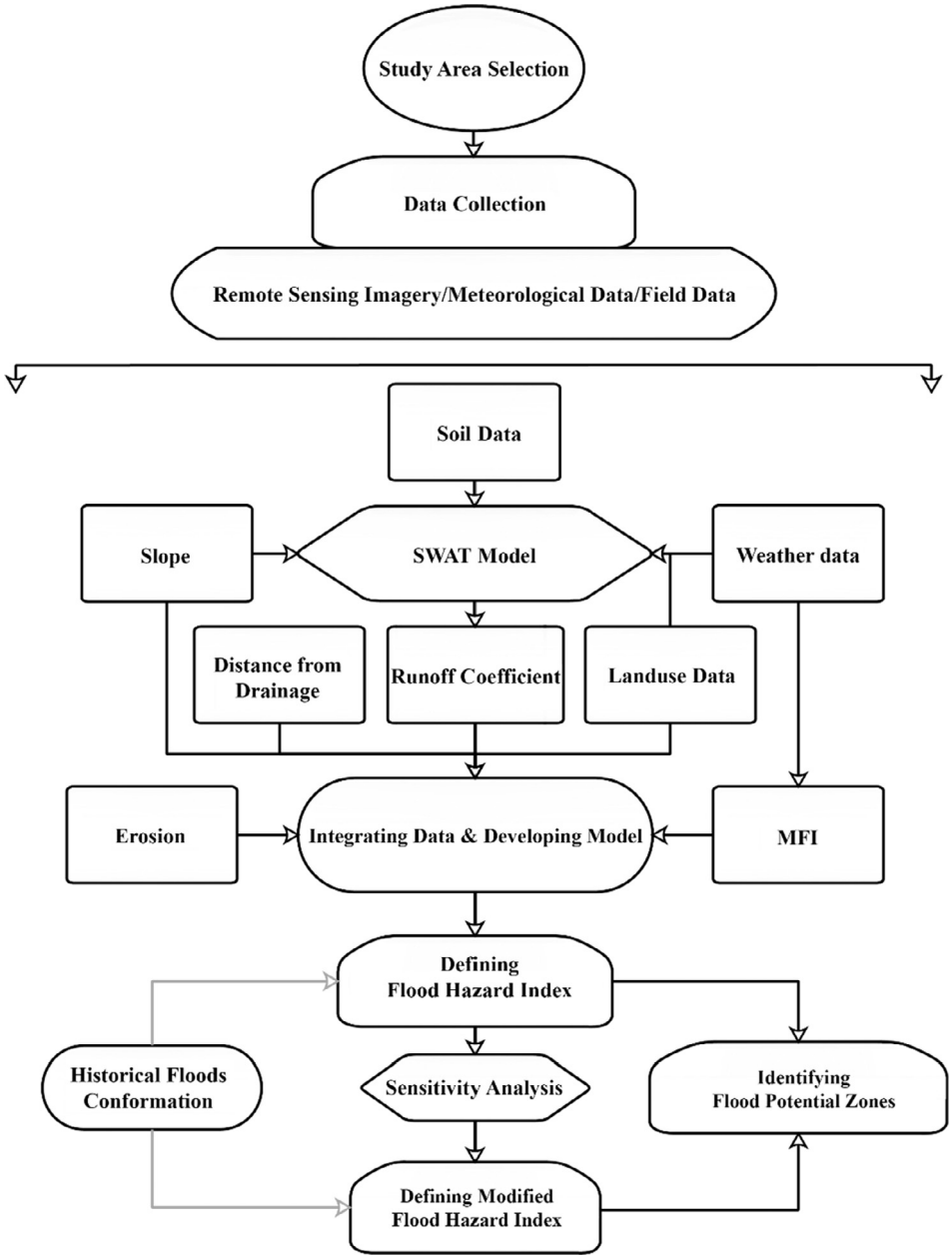

Fig. 1. Conceptual methodology framework used to identify flood hazard zones.

The definition of the criteria used in the Eq. (1) can be find in Table 2. It should be noted that i represents value of the criterion for each pixel.

2.3.1. Decision support system

To produce the flood hazard map Analytic Hierarchy Process (AHP) was used over a variety of MCDA techniques to generate a flood model of the area (Saaty and Vargas, 2001). AHP has been widely used in different MCDA frameworks due to their simple implementation and interpretation, as well as the consistency of the results despite redundancy of the data (Chen et al., 2013b; Chen et al., 2010; Dewan et al., 2007; Wang et al., 2011). Proper weights were assigned for the selected thematic layers in a scale from 1 to 9 suggested by Saaty (1980). Once the weights of the criteria were selected, a pair-wise comparison of the assigned weights matrices was constructed using Saaty's Analytic Hierarchy Process. Subsequently, these assigned weights were normalized by the eigenvector technique (Saaty and Vargas, 2001) and finally tested for consistency by computing a consistency ratio using Eq. (2) (Saaty, 1980):

$$\textit{Consistency ratio } (CR) = \frac{\lambda_{max} - n}{n - 1} \quad (2)$$

where, λ_{max} = Principal eigenvector computed by the eigenvector technique; n = number of criteria or factors

2.4. Data processing and analysis

In order to provide a realistic model that can be applied in remote regions, where data availability is limited, the SWAT model was used (Kundu et al., 2017). Using the SWAT model allows the combination of diverse flood generation contributing factors and reduces the likelihood of bias involved in GIS-based multi-criteria analysis. Although the index is based on the specific characteristics of MPB, it can be modified and applied in other regions. The spatial data was used as input for the SWAT computer software to determine the boundaries of basins and sub-basin as well as other relevant hydrological information to obtain a

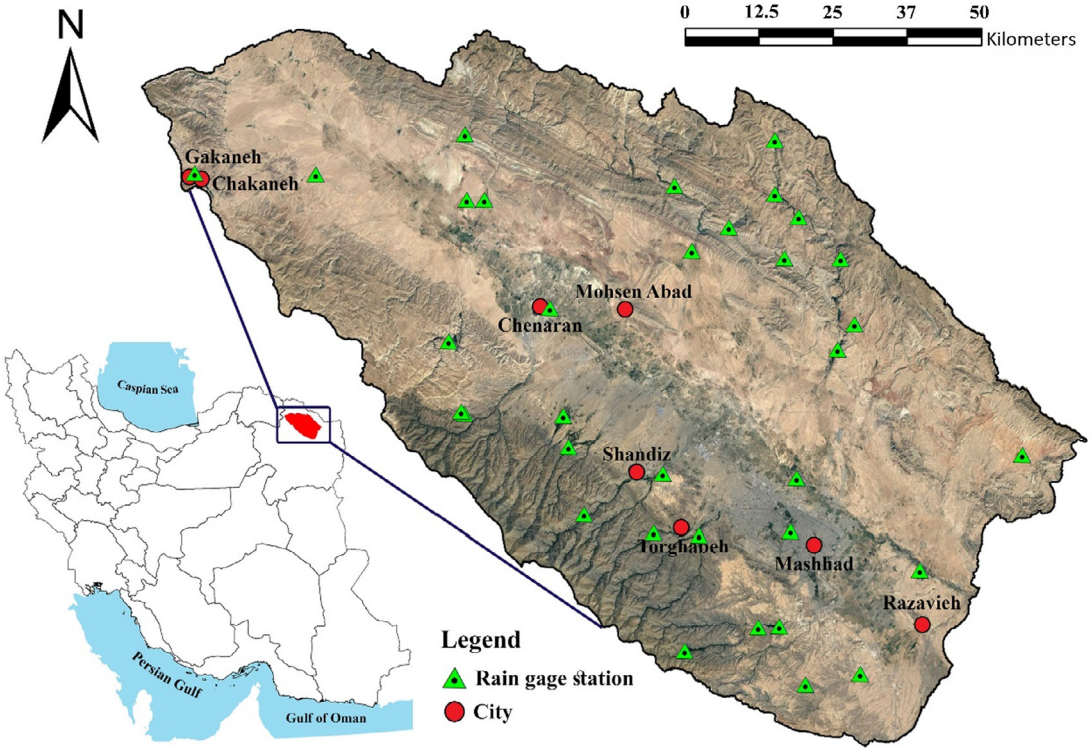

Fig. 2. Map showing Mashhad Plain Basin (MPB) located in Khorasan Razavi province, North-East of Iran.

Hydrological Response Unit (HRU). The combination of both spatial data and weather data supports the main basin model setup. The model was then ready for the simulation run. The initial validation process consisted in comparing the observed data with the rain-runoff model results. Since not enough data was available for the site, no calibration was performed due to the high level of uncertainty with a small sample, which is addressed through the sensitivity analysis explained in Section 2.5. Subsequently, a runoff coefficient was determined from a total of 43 sub-basins within the study area (Kundu et al., 2017; Shi et al., 2011). Additionally, the elevation and slope maps were generated in ArcGIS using the ASTER DEM surface and 3D Analyst tool. To calculate the distance from a river or stream, river polyline network layers and every pixel in the site, a raster map representing the study area was prepared. The distance from any point to a stream or river is calculated using Euclidean relation (Chen et al., 2015; Kazakis et al., 2015a).

In order to determine the Rainfall intensity (R) factor, the monthly rainfall data of 33 rain gauge stations were collected from Iran Metrological Organization (IRIMO) for 24 years from 1991 to 2015 (IRIMO, 2016). The spatial distribution of these stations is shown in Fig. 2. Then, the rainfall intensity (R) map was developed based on the Modified Fournier Index (MFI) using Eq. (3) (Morgan, 2005).

$$MFI = \sum_{i=1}^{12} \frac{P_i^2}{P} \quad (3)$$

where P_i is the monthly average amount of precipitation for month i (mm), and P is the average annual precipitation (mm).

MFI can be used to evaluate the land susceptibility to erosion by calculating the erodibility of land and soil losses and also in assessing land susceptibility to sliding (Aghiruş, 2010; Costea, 2012). The rainfall erosivity classes was determined by the MFI methodology for the present study. Previous have made use of this index successfully to provide a summary assessment of the probability of rainfall with significant erosive effects (Costea, 2012). Having calculated the MFI for each station, in order to obtain MFI for the whole study area, the results were then interpolated using the kriging method in ArcGIS environment. No topographic control to manage orographic rainfall effects was performed due to the high number of weather stations in the area, and the homogeneous distribution of elevations from the boundary, and towards the middle of the basin. Soil erodibility is a factor that exerts a great impact on flood-flow hydrographs, as well as the damages related to it, such as large sediment yields at flash floods (Kourgialas and Karatzas, 2017b). Since the existing land use and erosion data for the site was merely descriptive, to avoid data inconsistency, RS methods

Table 1
Data used in this research and their sources.

Data name	Detail	Sources
Rainfall	Excel File (1991–2015)	Iran Metrological Organization (IRIMO)
	Excel File (1982–2014)	Global Weather CFSR Data
Historical flood events	Excel File (1972–2014)	National Soil and water research institute of Iran Ministry of Agriculture
		Water Resources Department of the Prefecture of Mashhad
Drainage network map	1:250,000	Mashhad Spatial Data Infrastructure (SDI)
Soil erosion map	1:250,000	National Soil and water research institute of Iran Ministry of Agriculture
Soil map	Raster file	Harmonized World Soil Database v 1.2
Land use map	1:250,000	National Soil and water research institute of Iran Ministry of Agriculture
		Landsat data
ASTER DEM	30 m	United States Geological Survey (USGS) (2011)

Table 2
The most common criteria that have been used for identifying flood hazard areas.

Thematic layer	Abbreviation	Authors
Runoff coefficient	R	Current study
Elevation	E	(Chen et al., 2015; Fernández and Lutz, 2010b; Kazakis et al., 2015a; Kourgialas and Karatzas, 2016; Kourgialas and Karatzas, 2017a; Papaioannou et al., 2015; Tehrany et al., 2013; Tehrany et al., 2014a; Tehrany et al., 2015; Xiao et al., 2017)
Slope	S	(Chen et al., 2015; Fernández and Lutz, 2010b; Kazakis et al., 2015a; Kourgialas and Karatzas, 2016; Kourgialas and Karatzas, 2017a; Papaioannou et al., 2015; Tehrany et al., 2013; Tehrany et al., 2014a; Tehrany et al., 2015; Xiao et al., 2017)
Distance from the drainage network	D	(Chen et al., 2015; Fernández and Lutz, 2010b; Kazakis et al., 2015a; Papaioannou et al., 2015; Tehrany et al., 2014a; Tehrany et al., 2015; Xiao et al., 2017)
Rainfall intensity	RI	(Kazakis et al., 2015a; Kourgialas and Karatzas, 2016; Kourgialas and Karatzas, 2017a; Papaioannou et al., 2015; Tehrany et al., 2013; Tehrany et al., 2014a; Tehrany et al., 2015)
Soil erosion	ER	(Kourgialas and Karatzas, 2017a)
Land use	L	(Fernández and Lutz, 2010b; Kazakis et al., 2015a; Kourgialas and Karatzas, 2016; Kourgialas and Karatzas, 2017a; Tehrany et al., 2013; Tehrany et al., 2014a; Tehrany et al., 2015; Xiao et al., 2017)

(satellite images) and the traditional geological field mapping were applied to check their validity and update them before inserting in the model.

Having prepared thematic layers, selected weights (from 1 to 10) to be assigned to each factor features, the final map was further classified in different categories. All the above-mentioned key factors were finally normalized according to the AHP and eigenvector techniques and overlaid in Eq. (1). For all the factors except distance from drainage network and soil erosion and land use, the Jenk Natural Breaks (Chen et al., 2013a; Jenks, 1967) method was applied to establish different flood hazard levels, establishing the number of classes for each factor based on engineering expertise and judgement (Jenks, 1967). The Jenks natural breaks classification method may also be used which consists in clustering data to determine the best arrangement of values into classes, by minimizing the average deviation from the class mean while maximizing the deviation from the means of the other groups for each class (Jenks, 1967). However, it is recommended to evaluate any statistical approach with expertise judgement, and any historic flood data available, given that distributions may differ from reasonable values, specifically with the slope angle and distant from a cell in the model to a reach or river within the basin (Demek, 1972).

2.5. Validating results

Measuring the reliability of the criteria and robustness of the methodology is key to obtain realistic outputs, therefore, it is imperative to conduct validation procedures to test the results. Because of the high level of uncertainty of the field data gathered for the model due to the little amount and difficulty faced during the measurements required to obtain various parameters, these inputs may sometimes lead to high variability of outputs (Lenhart et al., 2002). Therefore, sensitivity analyses are required to reduce the uncertainty within the model (Kundu et al., 2017; Kushwaha and Jain, 2013). These analyses are suitable techniques to identify the implications of each parameter towards flood hazard analysis, since sensitivity analysis reduces the subjective perspective of various criteria, providing numerical results and help make decisions on weighting values assigned to each criterion. The single parameter analysis was introduced by Napolitano et al. (1996) in a different case scenario to estimate the contamination vulnerability of aquifers in several studies (Kazakis et al., 2015a). Another single-parameter sensitivity analysis manages the over-parameterization that usually occurs in hydrological modelling (Box and Jenkins, 1976; Kundu et al., 2017). Sensitivity analyses were conducted for each factor, and were implemented to calculate the basin's risk of flood (Napolitano and Fabbri, 1996). The sensitivity analysis method replaces the indexes used for the AHP with "effective weights" calculated using Eq. (4):

$$W = \frac{F_i \times F_w}{V} \times 100 \quad (4)$$

Where: W = the effective weight of each factor, Fi the factor i features value, Fw = the factor weight, V = the aggregated value of the applied index. The sensitivity analysis was then applied to all seven factors assumed to generate the mFHI map.

From the sensitivity analysis, the effective weights (Table 3) are then applied to obtain the modified Flood Hazard Index (mFHI). The mFHI index assumes the same class rating and parameters as the FHI, but using different weight values. The difference between mFHI and FHI lies in the sensitivity analysis applied to assign the new weights, thus improving the reliability of the results. Finally, these results were validated against 42 years of recorded flooding data.

3. Results and discussion

3.1. Flood hazard index (FHI)

The identification of the flood prone areas was undertaken using an AHP based multi-criteria decision analysis approach, which consists of determining the weights of the selected thematic layers (Fig. 3). The procedure of weighting thematic layers was set such that the consistency ratio for all of the obtained thematic layers was less than the limited threshold (0.10), to guarantee the consistency of the analysis (Saaty, 1980). According to the range of values obtained for these criteria, relative proper weights were assigned to different layers and their associated features. The methodology followed in this paper is simple and focused on those variables that would exceed the drainage-system capacity due to high peak flows. The selected flood criteria factors, as well as the corresponding weights assigned are shown in Table 3. Their selection was based on assumed values by experts in the field such as hydro-geologists, hydro-agronomists, environmentalists, and literature review (Kourgialas and Karatzas, 2011; Kourgialas and Karatzas, 2016; Kourgialas and Karatzas, 2017a; Sinha et al., 2008; Xiao et al., 2017; Zhao et al., 2018). The amount of water flow and its intensity depend on the characteristics of the basin, especially its land use, shape, size, and the weather conditions preceding to a rainfall occurrence (season and antecedent moisture condition) controlling the amount of rainfall that can permeate into the soil. These parameters vary from one site to another; thus, it is very important to carefully select appropriate and realistic values.

3.1.1. Runoff coefficient

Based on the initial hypothesis and the sensitivity analysis output results of Table 3, the most contributing factor towards high flood hazard levels is the runoff coefficient. In order to calculate the runoff coefficient, a 35-year average annual runoff (1982–2016) was used which shows the amount of water flowing through the sub-basins.

Table 3
Weights of the thematic layers and their features.

Thematic Layer (Factor weight)	Feature class	Assigned weight	Normalized weight
Runoff Coefficient			
(0.294)	0.031–0.041	2	0.07
	0.042–0.058	4	0.13
	0.059–0.087	6	0.20
	0.088–0.12	8	0.27
	0.13–0.18	10	0.33
Elevation			
(0.213)	856–1193	10	0.33
	1193.01–1499	8	0.27
	1499.01–1857	6	0.20
	1857.01–2264	4	0.13
	2264.01–3247	2	0.07
Slope			
(0.174)	0–5.05	10	0.36
	5.06–12.3	8	0.29
	12.4–20.8	5	0.18
	20.9–31.9	3	0.11
	32–80.4	2	0.07
Drainage Distance			
(0.118)	0–500	10	370
	500.1–1000	8	296
	1001–2000	5	185
	2001–5000	3	111
	5001–13,590	1	37
Rainfall Intensity (MFI)			
(0.089)	24.1–30.6	2	0.07
	30.7–34.8	4	0.14
	34.9–39.8	6	0.21
	39.9–48.5	8	0.28
Erosion			
(0.064)	Very low to low	2	0.11
	Moderate	6	0.33
	High to very high	10	0.56
Land use			
(0.048)	Semi-dense forest	2	0.04
	woodland and Scrubland	3	0.07
	Planting forests	4	0.09
	Scatter forest	5	0.11
	Dry Farming, Irrigated cropland	6	0.13
	high density pasture	7	0.16
	low and semi-dense pasture	8	0.18
	urban and built-up land, water bodies	10	0.22

Higher values of runoff coefficient indicate higher runoff and areas of concentrated flow, and consequently higher potential of flood to occur. The runoff coefficient values vary in a range between 0.031 and 0.18, with the highest values occurring in the Northern part of study area. When rainfall occurs over a catchment, and runoff begins to flow through it, several factors determine the amount of rainfall that will flow downhill and how fast it will travel. Furthermore, a percentage of the rain that falls on a basin is captured by vegetation and soil, and the remainder is routed through waterways as flow (Alaghmand et al., 2014; Bathrellos et al., 2017). Rivers and streams are also key hydrological units to convey storm water. The depth of water over the reach or stream will depend upon the geometry characteristics, vegetation cover, and the characteristics of obstacles found on their path.

3.1.2. Elevation and slope

Due to the fact that water flows in the direction of gravity, runoff and infiltration will be heavily influenced by the topography of the basin. Slope has a direct impact on runoff generation and transformation from rainfall to runoff. As the slope angle increses, the runoff generation increases and is conveyed towards areas with milder slopes. Areas at lower elevations downstream with flat slopes are more likely to be flooded compared to areas in higher elevation with steep slopes. The study area is surrounded by mountains and high elevation areas. Low-elevation areas are present in the central and south-east portions of the basin. The slope map is shown in Fig. 3. On average, about 51% of study area has slopes angles ranging around 0–5.05° and 22% between 5.06 and 12.3°. These figures for slopes range from 20.9 to 31.9°, ranged around 15% and 9%, while only 3% of study area is located on slope angles greater than 32°. The study area is surrounded by mountain ranges at the North and South of the basin, containing steep slopes, while the central part has in general a mild slope which results in higher vulnerability to flood events. By simple observation, low slope and low elevation areas have been assigned the highest hazard weight rating, as prone areas (Table 3). Slope and elevation are not the only most flood-hazard important factors, but they are considered reliable criteria because they are derived from the ASTER DEM. They can finely discriminate land units to delineate areas of different hazard levels for a detailed assessment. These two indices accordingly received higher weights. DEM. They can finely discriminate land units to delineate areas of different hazard levels for a detailed assessment. These two indices accordingly received higher weights.

3.1.3. Distance from drainage network

When modeling flood, river-overflows play a critical role in the initiation of a flood event.

When the volume of water exceeds the drainage capacity of the streams in the area, the water depth will increase in low-lying areas leading to waterlogging. Often the inundation emanates from riverbeds and expands to the surroundings. The farther the location of a site to a river bed, the lower the risk of flood. Therefore, distance from the drainage network has been considered as the third most influential factor in the methodology. The classes of this criterion have been defined according to historical floods that took place in different parts of the world. It has been found that areas near the river network (< 500 m) are considered highly flood prone areas, whereas the effect of this parameter decreases in distances > 2000 m (Fig. 3 and Table 3).

3.1.4. Rainfall intensity

The monthly data used to estimate the rainfall intensity is not always applicable for flood hazard analysis. However, they were considered acceptable due to the number of meteorological stations around the MPB, with a 24-year record which is considered a reasonable record length compared to other nearby sites. It is relevant to mention that the present method requires a classification into five categories of hazard level, and therefore, does not require rather accurate rainfall data. The rainfall intensity was determined by using the modified Fournier index (Costea, 2012; Scrinzi et al., 2006). In this study, monthly rainfall data of 33 rain gage stations, located on MPB, were collected from the Iran Metrological Organization (IRIMO, 2016) for the 24-year period ($1991-2015$). For the present study, MFI ranges from 24.1 to 48.5 (Table 3), with the higher values located in the southern part and northcentral part of the study area (Fig. 3). The modified Fournier index (MFI) was used to classify the erosivity index at MPB, resulting in low erosion hazard class (< 60) (Costea, 2012). It was observed that the index calculated presented an intermittent trend, varying yearly (Costea, 2012). Despite the variations between years, the mean annual erosivity index classified the site into a low erosion hazard zone (Fig. 3). Since rainfall intensity is associated both with the frequency and the amount of precipitation, it is crucial to consider both values (Ouma and Tateishi, 2014; Tehrany et al., 2014a).

3.1.5. Soil erosion

The geological characteristics of the study area heavily influence the flood hazard index. However, they were not considered directly in the calculation, because they can be incorporated into the SWAT model

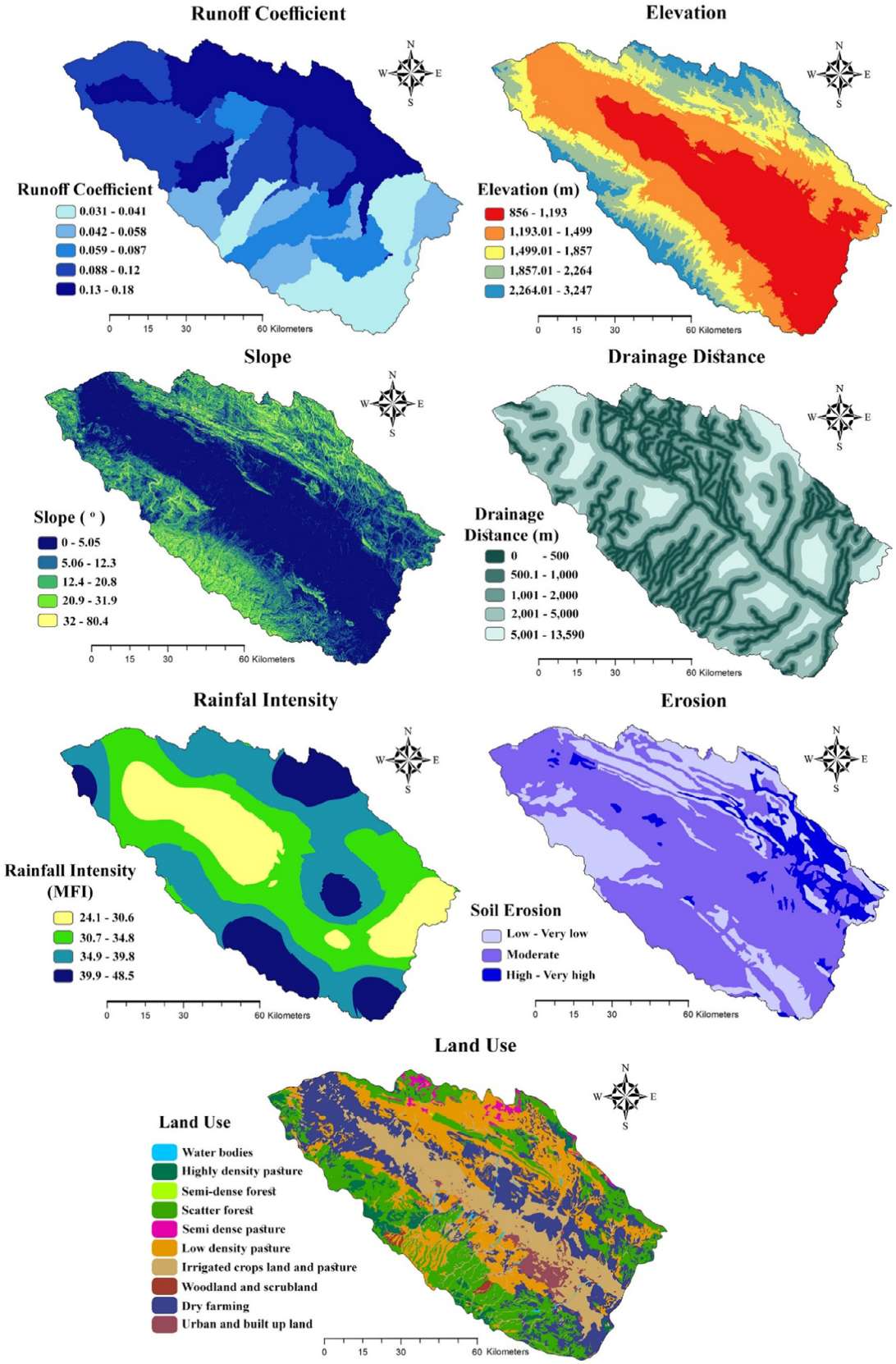

Fig. 3. Input layers in GIS environment and their associated features.

indirectly. The presence of high erosivity of soils increases the risk of flooding, particularly during heavy rainfall intensities. Therefore, after rainfall intensity, this factor was considered the next most relevant factor. The original data related to the soil erosion of MPB was obtained from the National Soil and Water Research Institute of Iran Ministry of Agriculture (NSWRI, 2016).

Soil erodibility can be obtained from average annual records of soil profile reaction to processes of detachment and transport of particles as a result of runoff and raindrop impact (Kourgialas and Karatzas, 2017a; Panagos et al., 2012). The rate of detachment of soil particles is mainly a function of the cohesivity of the soil. The ability to hold water controls the amount of runoff present in cohesive soils, while less cohesive soils have less capacity, and thus represent a higher flood risk. In addition, higher sediment yields present in the runoff or flow often occur on less cohesive soils, which results in higher peak flow rates and subsequently causes more damage through flash floods (Cazemier et al., 2001; Chang et al., 2010; Kourgialas and Karatzas, 2017a; Ni et al., 2003) (Table 2).

3.1.6. Land use

The behavior of the relationship between rainfall and the resulting runoff and groundwater, as well as the flow of debris, depends heavily on the land use characteristics of the site (NSWRI, 2016). Forests and dense vegetation covered areas increase the amount of water infiltration and abstractions, while urban and pasture covered areas augment the amount of overland flow. The land use is considered the least important factor in the present study, since the effect of land use was intrinsically considered in SWAT model to calculate the average runoff coefficient.

Different classes of land use and the associated percentage are presented in Table 3 and the land use map is shown in Fig. 3. The map analysis shows that 25% of the basin area consists of dry farming, 24% of semi-dense pasture, 23% of low-density pasture and about 19% of irrigated agriculture and gardens (Table 3). In the urban and rural sector, some intensive human practices may increase the risk of flood, resulting in the likelihood of damage and losses. These changes may be reflected through land use information and thus can be taken into account for the calculation of the hazard index.

3.2. Flood hazard mapping

The final output flood hazard map was developed by combining the defined factors and now is illustrated in Fig. 4. The output classes were defined based on the linear combined data derived from information provided by the model described previously. The FHI ranges around 0.101–0.356 and based on these results, the study area was categorized into five potential hazard zones representing: (a) 'Very Low' (FHI = 0.101–0.187), (b) 'Low' (FHI = 0.188–0.220), (c) 'Moderate' (FHI = 0.221–0.249), (d) 'High' (FHI = 0.250–0.279), and (e) 'Very High' (FHI = 0.280–0.356) flood potential hazard. The 'Very High' and 'High' flood hazard sites spread almost over the central part of study area, specifically in the northwestern, southeastern, and center portions of the basin, covering an area of 1180 (12%) and 2696 km^2 (28%) of total area, respectively. Moreover, 2700 km^2 (28%) of the MPB is subject to 'Moderate' flood hazard and are mainly distributed around the central portion of the study area. Subsequently, a surface area of 2216 km^2 (23%) and 893 km^2 (9%) lie within low and very low flood hazard potential areas respectively. the 'Low' and 'Very Low' hazard potential areas comprise a major portion of the eastern and western part of the study area. The results clearly show a significant percentage (40%) of areas in MBP are under "Very High" or "High" flood hazard.

The areas labelled in the map as high flood hazard are strongly influenced by the runoff coefficient courses according to the high weight given to this factor in the model. The final map shows that the MPB has the highest flood hazard over an extended area as a consequence of the combination of lowlands with slopes under 5°. Table 4 shows the flood hazard areas and the corresponding percentage for each

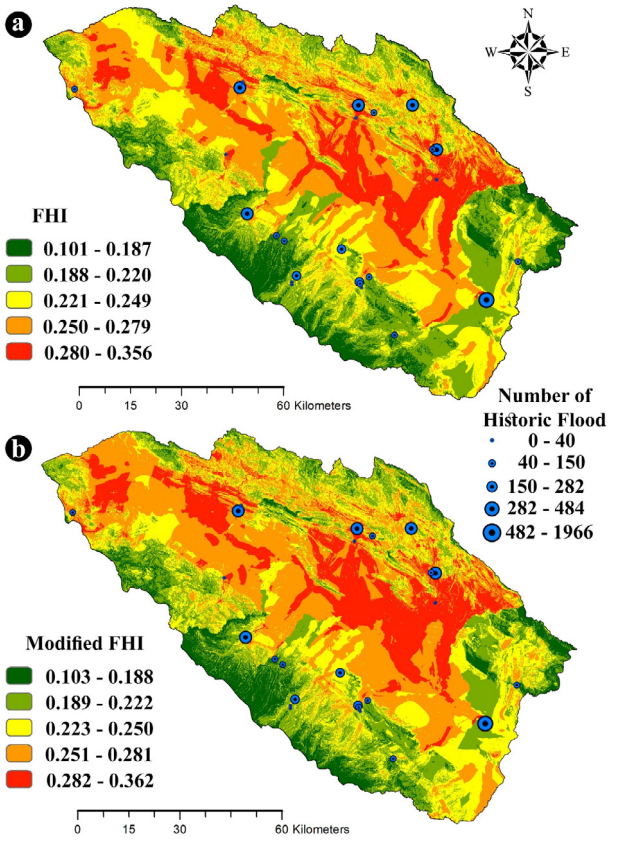

Fig. 4. Flood hazard maps: a) Flood hazard index and b) modified flood hazard index.

of land uses. According to the land use maps overlaid on the flood hazard output map; 43, 30 and 18% of the very high flood hazard zones are located in dry farming, irrigated cropland and pasture, and low-density pasture areas respectively. Likewise, the majority of high-flood hazard areas are Dry Farming, Irrigated cropland and pasture, and low-density pastures, followed by semi dense pastures and urban areas, whereas irrigated cropland and pasture and Dry Farming represent 31 and 29% of this zone. Very low flood prone areas appear mainly at woodland and Shrub land, and in high density pasture areas. Breaking it down into land use classification, 43.24% of high-density pasture, 36.29% of semi-dense pasture, 38.11% of woodland and Shrub land, 36.41% of Scatter forest, and finally 30.85% of Semi-dense forests of MPB are under low flood hazard, while 42.55% of scatter forests, 48.45% of semi-dense forest and 33.71% of low-density pasture are under moderate flood hazard.

The map shows very high flood hazard areas located at extended urbanization areas such as Mashhad city. The forests, and high-density pastures with the lowest percentages of very high and high flood hazard lie in the relatively safe region from which seven are found within the low hazard zone and three in the safe zone.

The FHI map revealed the importance of streams and tributaries in flood events. FHI indicates that riverbeds in the lowland are even more prone to flood. Other similar studies have identified a direct relationship between agricultural land management and the behavior or flooding at the sub basin level (> 10 km^2) (Kourgialas and Karatzas, 2017a; O'Connell et al., 2007). Land use management heavily influences the impact of flood peak delay in intermediate and lower elevation areas, especially during moderate rainfall events. These measures are key to alleviate flooding by retaining and capturing rainfall during a storm and subsequently reducing the time of flood warnings (Salazar et al., 2009). At MPB there is a large number of crops located primarily at the intermediate and low elevation areas. These locations represent

Table 4
Distribution of land use in flood hazard areas.

Land-use class	Area (km^2)	%	Overlapping percentage with Different hazard Levels				
			Very low	Low	Moderate	High	Very high
Water bodies	34.70	0.36	0.12	22.36	32.44	22.49	22.59
Rock protrusions	15.92	0.16	9.87	26.37	17.77	12.26	33.63
Woodland and shrub land	50.29	0.52	37.50	38.11	15.11	5.52	3.74
Scatter forest	113.32	1.17	3.38	36.41	42.55	16.41	1.16
Semi-dense forest	2.72	0.03	0.29	30.85	48.45	19.35	0.41
Planting forests	1.16	0.01	0.00	0.00	0.00	57.04	42.96
Irrigated cropland and pasture	1844.88	19.03	0.91	12.24	22.04	45.26	19.55
Dry farming	2446.19	25.23	2.58	16.79	27.53	32.34	20.74
Low density pasture	2293.69	23.66	8.01	22.45	33.71	26.32	9.50
High density pasture	322.47	3.33	33.09	43.24	20.85	2.54	0.21
Semi-dense pasture	2317.40	23.90	21.51	36.29	26.50	12.71	2.93
Urban and built-up land	253.65	2.62	0.02	4.08	37.22	51.87	6.81
Total	**9696.38**	**100**	**9**	**23**	**28**	**28**	**12**

an interesting target for the implementation of appropriate land use practices and policies at the national scale to assess flooding, such as the enhancement of the infiltration capacity through changes in vegetation cover and the runoff flow connectivity through the system. It is recommended to accompany these types of preventive measures, with a flood warning system at the river basin scale. Weather stations may be used to provide real time hydro-meteorological information to provide early flood warnings (Kourgialas and Karatzas, 2011; Salazar et al., 2009). The information would also provide a measurement of the threat and the procedures to be applied accordingly by government agencies. These findings provide insight towards flow mitigation plan and preventive action, as well as a guide to adaptation approaches for agricultural and urban land use practices to minimize flood damage caused by human impact on the landscape, and climate change (Blackwell et al., 2006; Morris et al., 2010; Thieken et al., 2007).

3.3. Validation — sensitivity analysis

The weight factors and their associated feature classes thresholds of the model input have a crucial impact on the evaluation of the results. Since their determinations were significantly influenced by the interpretations of experts, the selection of the flood hazard areas can be sensitive to changes in the decision weights associated with the criteria (Chang et al., 2008; Fernández and Lutz, 2010a) based on the judgement of the experts. To address this issue, a sensitivity analysis was conducted, where layer weights values were varied to evaluate the differences in the final result. Initially, FHI considered the runoff coefficient as the dominant parameter. Elevation and slope angle respectively were considered the next significant parameter, and followed by rainfall intensity, soil erosion and land use. Surprisingly, the sensitivity analysis concluded that the order of influence of these factors in the studied region is identical to the FHI. This confirms the high accuracy of the proposed method. However, some calculated factors had slight differences (Table 5). The results of the sensitivity analysis also showed that the least sensitive factor was land use, which was expected due to the weight factors assigned (Tehrany et al., 2014b) (Table 3).

Table 5
Statistics of the effective weights-sensitivity analysis.

Parameters	Initial weight	min	max	mean (μ)	SD (σ)
Runoff coefficient (R)	0.294	0.071	0.580	0.270	0.111
Elevation (E)	0.213	0.050	0.511	0.217	0.072
Slope (S)	0.174	0.043	0.412	0.207	0.062
Drainage distance (D)	0.118	0.015	0.318	0.097	0.055
Rainfall intensity (RI)	0.089	0.023	0.353	0.096	0.048
Soil erosion (ER)	0.064	0.023	0.238	0.079	0.036
Land use (L)	0.048	0.007	0.085	0.033	0.009

The mFHI map and FHI map are very similar, however, FHI underestimates the hazard level at the tributaries and reaches located at the center of the MBP, whereas the sensitivity analysis conducted with the mFHI classified these areas as high-flood hazard potential. Despite these differences, as shown in Fig. 4a and b, the sensitivity analysis results coincide with the FHI outcomes in general. The analysis performed comparing both FHI and mFHI, reveals relevant data regarding the weight of each parameter and how they affect the outcome of the flood hazard classification.

Land use was assigned the smallest weight, partly due to the almost uniform values across the region (Tehrany et al., 2014b). However, the effect of land use is especially critical to urban areas where the population is high. It is relevant to note that land use is also taken into account within the SWAT model and would heavily influence the runoff coefficient factor. Additionally, the distance from drainage produced relatively significant impacts on the resultant hazard map, which can be clearly observed particularly in the north-west area.

In order to verify the final flood hazard map, a review of historical flooding on MBP was introduced (Diakakis et al., 2012; Kourgialas and Karatzas, 2016). As shown in Fig. 4, the legend shows black dots representing the locations where historical floods occurred, with green dots around each, representing the number of occurrences of flood on each location. The size of the green dots indicates the number of occurrences, the bigger the circle, the greater the number of occurrences. It is noted in this diagram how most of the historic record flood points appear on the eastern portions of MPB. In order to validate the final output flood hazard map in accordance to the historical flood records, the “Extract by Mask” tool was applied using GIS. The cells of the flood hazard raster map were extracted exactly where the coordinates of the historical flood records were located. Through this method it is possible to identify which flood hazard index classification corresponded to each of the flood record points. Additionally, the number of the flooded points that were located in each flood hazard area was determined. Based on the above procedure, for the final flood hazard map, almost all the recorded historical floods took place at the moderate to very high

Table 6
Classes of flood hazard and number of historical flood events.

Hazard Level	FHI			mFHI		
	Area (%)	Number of events	%	Area (%)	Number of events	%
Very low	9	113	2	9	113	2
Low	23	53	1	21	53	1
Moderate	28	3093	57	25	2993	55
High	28	711	13	30	811	15
Very high	12	1437	27	16	1437	27

flood hazard areas with only 3% of them in areas of low flood hazard.

Records of historical flood events support the indications of the mFHI analysis through the recurrent flooding of MPB. As shown in Table 6, mFHI analysis classifies as highly susceptible areas with a high number of recorded flood events in very high and high classes, an additional indication of the accuracy of the proposed methodology.

According to Table 6, for both FHI and mFHI maps, more than 97% of historical flood events have occurred in moderate to very high, and 27% at very high flood hazard locations which represent 12% of the total MPB total area. The consistent matching between the flood hazard map and the historic flood point records not only occurs at low and semi-mountainous locations, but also at the mountain plateaus of MPB. In Fig. 4 a comparison between FHI and mFHI in terms of number of events demonstrates that the FHI underestimates high and very high flood hazard areas. Several locations of historical records of flood with high levels of occurrence have been found to be assessed by the mFHI while FHI had underestimated with low classification indexes. Additionally, the sensitivity analysis results revealed that very high and high-flood hazard ranking zones represented 16% and 30% of the entire MBP, while the FHI estimated 12% and 28% respectively. It has also been observed that the FHI overestimated areas that were ranked as low and moderate flood hazard through the presented method.

3.4. Discussion of proposed methodology

A detailed review by Birkholz et al. (2014) highlighted the necessity to reformulate the perception of flood hazard in research work, to develop a more integrated and comprehensive approach of how risk perceptions influence the capacity, resilience and vulnerability of individuals and communities against flood.

Due to the research advances and increasing computational and data resources, there is a large gap between large-scale approaches and detailed reach scale hydraulic models (Sampson et al., 2015). Large-scale flood modeling approaches have recently begun to include hydrological modeling components to provide more accurate flood mapping (Dottori et al., 2016).

The present study incorporates SWAT as an accurate approach to help forecast flood events using a rainfall-runoff response that would enhance the behavior of the parameters of the basin, as well as reducing the uncertainty of the parameters used for the MCDA process to obtain the FHI index.

The main advantage of the FHI index is its ability to provide an overall assessment of flood hazard areas. The limitations of the FHI methodology are usually related to the requirements of the raw data, such as detailed topography, accurate and complete historic hydro-meteorological data, as well as up to date soil-land use information of the analyzed site. Even if all of these requirements are met, it only reduces the level of uncertainty of the flood hazard assessment. The proposed methodology, on the other hand, can be suitable where limited data is available, and the framework can be used to relatively prioritize vulnerable areas. The validation of the modeling results with historical flood events demonstrated the accuracy of the final results and confirmed that using hydrological modeling (SWAT) is reliable, flexible, and produces highly accurate results. Furthermore, in this study developed with SWAT model, requires minimum data that is available globally. It provides a comprehensive method to facilitate decision-making and offers a time-efficient and cost-effective method for the identification of flood prone sites. The intent of the present research study is to provide a methodology that relies non only on static index-based methodologies, but also incorporating an framework integrating hydrological models such as SWAT with MDCA using GIS tools. If the proposed mFHI methodology was to be used in other different regions, other weight values for each criterion factor would need to be assumed depending on the geophysical characteristics of the target site, which shows the main drawback of the method, relying heavily on the subjectivity of the weight values of each criterion. However, the single parameter sensitivity analysis proved to be a useful to evaluate the weights assumed.

As Table 6 shows, the proposed mFHI has proven to acquire similar results compared to FHI. The differences may lie in the fact that SWAT incorporates many of the contributing parameters in the model to obtain more accurate or realistic results. Previous examples of FHI work suggest different results in the ranking of the factors assumed, as well as different factors that were not included in the present study (Chen et al., 2015; Fernández and Lutz, 2010b; Papaioannou et al., 2015; Tehrany et al., 2013; Tehrany et al., 2014b; Xiao et al., 2017). For instance, Kourgialas and Karatzas (2016) and (Kazakis et al., 2015b) suggested flow accumulation had a major contribution towards hazard mapping. For the present work it was preliminarily included but it had proven to develop a small sensitivity towards the flood hazard results, and thus it was removed from the analysis.

Soil water retention was a major factor included by Chen et al. (2015), modeled using the SCS CN number method for runoff calculation, which requires soil, cover and land used altogether. The advantage of using SWAT includes all these factors, except that they interact independently in the rainfall-runoff model, providing more sensitivity to each of these factors and not relying on a single curve number parameter.

Distance to rivers and streams, as well as water table levels were important factors assumed for hazard assessment in the case of Fernández and Lutz (2010b). Since the data available for MPB had shown a decline in water table levels, this criterion was also removed from the analysis (NSWRI, 2016).

As shown in the previous similar works cited utilizing FHI methodology, the weight of parameter assumed for any basin will vary from site. MCDA problems are based on the specific characteristics of case study, but can be modified and applied in other regions accordingly. The present study considers the runoff coefficient as a factor for first time, modeled more accurately with SWAT, and has demonstrated its relevance towards flood hazard mapping. Previous work using MCDA have shown that land use may represent an important criterion (Kourgialas and Karatzas, 2011; Kourgialas and Karatzas, 2016; Kourgialas and Karatzas, 2017b). Although land use in our case presented little influence towards determining hazard levels because of the low weight values assumed, it may be misleading due to the fact that it may indirectly affect other parameters, in our case the runoff coefficient. The present study provides a baseline for future work to develop sensitivity analysis not only for the criteria factors assumed for the site, but also the influence of the same factors towards the hydrologic model.

Through the implementation of these models, a further step for future research work involves the estimation of peak flows corresponding to different exceedance probabilities at locations where the output map has identified high and very high flood hazard levels. The output information may provide local authorities and land development managers and stakeholders and farmers with a comprehensive tool to assess flooding in areas under risk of flood accordingly. It is recommended other future studies may use different weight criteria assumption methods to modify the proposed methodology. The applications of the FHI can be used to assess flood hazards in other locations. Coupled with validation methods, such as the sensitivity analysis, this methodology is able to provide reliable and accurate results. The present mFHI approach may prove helpful to evaluate global models at a large scale to reduce the over or under estimation of the flood hazards, using a rather simple GIS based tool which requires a relatively less expensive method to be applied even if the available data is scarce.

4. Conclusion

The purpose of the present study is to propose a methodology for flood hazard assessment that is transferable to different locations around the globe. The proposed model can be used for basin management, and for the development of flood prevention and mitigation plans

that may lead to a reduction of flood impact or damage caused by intensive precipitation. The method spatially analyzes seven parameters, combining the information in the Flood Hazard Index (FHI). The parameters are runoff coefficient (R), elevation (E), slope (S), distance from the drainage network (D), rainfall intensity (RI), soil erosion (SE) and land use (L). The weight of each parameter was calculated by using the Analytic Hierarchy Process, that consists of a sophisticated statistical analysis. The highest weight was assigned to the runoff coefficient and the lowest to land use. Flood hazard was classified in five categories ranging from very high to very low. The output values were validated by overlaying historical flood in the basin, as well as the development of a statistical sensitivity analysis on the values assigned to the different criteria to validate the accuracy and consistency of the developed methodology. The proposed modified method is named mFHI. The comparison of the flood hazard maps obtained with the FHI and mFHI indices indicate that both indices are reliable, however, it is necessary to use the historical flood records to test the consistency of the results in high- and very high-flood hazard areas. According to the results, 9% of the total area of study area is subject to very low flood hazard, while about 40%, is under very high or high flood hazard. Since flood events represent a major concern in study area, the presented methodology could provide insight for the identification of potential flood hazard areas and for improved and innovative water and risk management practices. Additionally, this study discussed and proposed a global flood hazard investigation framework for identifying very high flood risk areas. It is hoped that the developed methodology will benefit water management professionals engaged in climate change and natural disaster management planning scenarios across the globe, by providing sustainable development and resilience to extreme weather events.

Conflict of interest

No interests to declare.

Acknowledgments

The present article was financially supported by the Department of Civil Engineering of Monash University. The authors extend their sincere gratitude to Prof. Seyed Mahmood Hosseini who provided insight and expertise that greatly assisted the research. We would also like to express our deep gratitude to the editor and reviewers for their constructive comments and suggestions.

References

Aghiruş, C., 2010. Culmea şi piemontul Codrului, Rezumatul tezei de doctorat, Universitatea Babeş-Boliay, Cluj-Napoca, aerapa. conference. ubbcluj. ro/2012/pdf/42% 20COSTEA. pdf.

Al-shabeeb, A.R., 2016. The Use of AHP within GIS in selecting potential sites for water harvesting sites in the Azraq Basin—Jordan. J. Geograph. Inf. Syst. 8 (01), 73.

Alaghmand, S., Abdullah, R., Abustan, I., Said, M., Vosoogh, B., 2012a. GIS-based river basin flood modelling using hec-hms and mike 11-Kayu Ara river basin, Malaysia. J. Environ. Hydrol. 20.

Alaghmand, S., Beecham, S., Hassanli, A., 2014. Impacts of vegetation cover on surface-groundwater flows and solute interactions in a semi-arid Saline floodplain: a case study of the lower Murray river, Australia. Environ. Processes 1 (1), 59–71.

Alaghmand, S., Bin Abdullah, R., Abustan, I., Eslamian, S., 2012. Comparison between capabilities of HEC-RAS and MIKE11 hydraulic models in river flood risk modelling (a case study of Sungai Kayu Ara River basin, Malaysia). Int. J. Hydrol. Sci. Technol. 2 (3), 270–291.

Alaghmand, S., Bin Abdullah, R., Abustan, I., Vosoogh, B., 2010. GIS-based river flood hazard mapping in urban area (a case study in Kayu Ara River Basin, Malaysia). Asian J. Water Environ. Pollut. 2 (6), 488–500.

Anand, J., Gosain, A.K., Khosa, R., 2018. Prediction of land use changes based on Land Change Modeler and attribution of changes in the water balance of Ganga basin to land use change using the SWAT model. Sci. Total Environ. 644, 503–519. https://doi.org/10.1016/j.scitotenv.2018.07.017.

Bathrellos, G.D., Skilodimou, H.D., Chousianitis, K., Youssef, A.M., Pradhan, B., 2017. Suitability estimation for urban development using multi-hazard assessment map. Sci. Total Environ. 575, 119–134.

Birkholz, S., Muro, M., Jeffrey, P., Smith, H.J., 2014. Rethinking the relationship between flood risk perception and flood management. Sci. Total Environ. 478, 12–20.

Blackwell, M.S., Maltby, E., Gerritsen, A., 2006. Ecoflood Guidelines: How to use floodplains for flood risk reduction.

Box, G.E., Jenkins, G.M., 1976. Time series analysis: forecasting and control, revised ed. Holden-Day.

Bradford, A., Denich, C., 2007. Rainwater management to mitigate the effects of development on the urban hydrologic cycle. J. Green Build. 2 (1), 37–52.

Cazemier, D., Lagacherie, P., Martin-Clouaire, R.J.G., 2001. A possibility theory approach for estimating available water capacity from imprecise information contained in soil databases. Geoderma 103 (1–2), 113–132.

Chang, D., Zhang, L.J.N.H., Sciences, E.S., 2010. Simulation of the erosion process of landslide dams due to overtopping considering variations in soil erodibility along depth. Nat. Hazards Earth Syst. Sci. 10 (4), 933–946.

Chang, N.-B., Parvathinathan, G., Breeden, J.B., 2008. Combining GIS with fuzzy multicriteria decision-making for landfill siting in a fast-growing urban region. J. Environ. Manage. 87 (1), 139–153.

Chen, J., Yang, S., Li, H., Zhang, B., Lv, J.R., 2013a. Research on geographical environment unit division based on the method of natural breaks (Jenks), pp. 47–50.

Chen, Y., et al., 2015. A spatial assessment framework for evaluating flood risk under extreme climates. Sci. Total Environ. 538, 512–523.

Chen, Y., Yu, J., Khan, S., 2013b. The spatial framework for weight sensitivity analysis in AHP-based multi-criteria decision making. Environ. Modell. Software 48, 129–140.

Chen, Y., Yu, J., Khan, S.J., 2010. Spatial sensitivity analysis of multi-criteria weights in GIS-based land suitability evaluation. Environ. Modell. Software 25 (12), 1582–1591.

Chowdhury, A., Jha, M.K., Chowdary, V., 2010. Delineation of groundwater recharge zones and identification of artificial recharge sites in West Medinipur district, West Bengal, using RS, GIS and MCDM techniques. Environ. Earth Sci. 59 (6), 1209.

Costea, M.J., 2012. Using the Fournier indexes in estimating rainfall erosivity. Case study-the Secasul Mare Basin. Aerul si Apa. Componente ale Mediului 313.

CRED, 2009. Centre for Research on the Epidemiology of Disasters (CRED). EM-DAT: The International Disaster Database. Brussels, Belgium, Université Catholique de Louvain. http://www.cred.be/emdat/intro.html.

Dao, A., Han, M., Nguyen, V., Ho, X., Kim, T., 2009. Flooding mitigation plan at downtown of Hanoi by rainwater harvesting. Proceeding of UNESCO-IHP Session: Combining rain culture with rainwater harvesting technology for sustainable development in South and East Asia, 9th September.

Demek, J., 1972. Manual of Detailed Geomorphological Mapping. Academia.

Dewan, A.M., Islam, M.M., Kumamoto, T., Nishigaki, M., 2007. Evaluating flood hazard for land-use planning in Greater Dhaka of Bangladesh using remote sensing and GIS techniques. Water Resour. Manage. 21 (9), 1601.

Diakakis, M., Mavroulis, S., Deligiannakis, G.J.N.h., 2012. Floods in Greece, a statistical and spatial approach. Nat. Hazards 62 (2), 485–500.

Dottori, F., et al., 2016. Development and evaluation of a framework for global flood hazard mapping. Adv. Water Resour. 94, 87–102.

Fernández, D., Lutz, M., 2010a. Urban flood hazard zoning in Tucumán Province, Argentina, using GIS and multicriteria decision analysis. Eng. Geol. 111 (1), 90–98.

Fernández, D., Lutz, M.J.E.G., 2010b. Urban flood hazard zoning in Tucumán Province, Argentina, using GIS and multicriteria decision analysis. Eng. Geol. 111 (1–4), 90–98.

Gassman, P.W., Arnold, J.J., Srinivasan, R., Reyes, M., 2010. The Worldwide use of the SWAT Model: Technological Drivers, Networking Impacts, and Simulation Trends, 21st Century Watershed Technology: Improving Water Quality and Environment Conference Proceedings, 21–24 February 2010, Universidad EARTH, Costa Rica. American Society of Agricultural and Biological Engineers, pp. 1.

Grimaldi, S., Li, Y., Pauwels, V.R., Walker, J.P., 2016. Remote sensing-derived water extent and level to constrain hydraulic flood forecasting models: opportunities and challenges. Surv. Geophys. 37 (5), 977–1034.

Grimaldi, S., Li, Y., Walker, J.P., Pauwels, V.R.N., 2018. Effective representation of river geometry in hydraulic flood forecast models. Water Resour. Res. 54 (2), 1031–1057. https://doi.org/10.1002/2017WR021765.

IRIMO, 2016. Iran Metrological Organization https://www.irimo.ir.

Jajarmizadeh, M., et al., 2016. Prediction of surface flow by forcing of climate forecast system reanalysis data. Water Resour. Manage. 30 (8), 2627–2640.

Jenks, G.F., 1967. The data model concept in statistical mapping. Int. Yearbook Cartograp. 7, 186–190.

Jozaghi, A., et al., 2018. A comparative study of the AHP and TOPSIS techniques for dam site selection using GIS: a case study of Sistan and Baluchestan Province, Iran. Geosciences 8 (12), 494.

Kain, C.L., Rigby, E.H., Mazengarb, C., 2018. A combined morphometric, sedimentary, GIS and modelling analysis of flooding and debris flow hazard on a composite alluvial fan, Caveside, Tasmania. Sed. Geol. 364, 286–301. https://doi.org/10.1016/j.sedgeo.2017.10.005.

Kazakis, N., Kougias, I., Patsialis, T., 2015a. Assessment of flood hazard areas at a regional scale using an index-based approach and Analytical Hierarchy Process: application in Rhodope–Evros region, Greece. Sci. Total Environ. 538 (Supplement C), 555–563. https://doi.org/10.1016/j.scitotenv.2015.08.055.

Kazakis, N., Kougias, I., Patsialis, T., 2015. Assessment of flood hazard areas at a regional scale using an index-based approach and Analytical Hierarchy Process: application in Rhodope-Evros region, Greece. Sci. Total Environ. 538, 555–563.

Khorrami, M., et al., 2019. How groundwater level fluctuations and geotechnical properties lead to asymmetric subsidence: a PSInSAR analysis of land deformation over a transit corridor in the Los Angeles Metropolitan Area. Remote Sens. 11 (4), 377.

Kourgialas, N.N., Karatzas, G.P., 2011. Flood management and a GIS modelling method to assess flood-hazard areas—a case study. Hydrol. Sci. J. 56 (2), 212–225.

Kourgialas, N.N., Karatzas, G.P., 2016. A flood risk decision making approach for Mediterranean tree crops using GIS; climate change effects and flood-tolerant species. Environ. Sci. Policy 63, 132–142.

Kourgialas, N.N., Karatzas, G.P., 2017a. A national scale flood hazard mapping

methodology: the case of greece-protection and adaptation policy approaches. Sci. Total Environ. 601, 441–452.
Kourgialas, N.N., Karatzas, G.P., 2017b. A national scale flood hazard mapping methodology: the case of Greece – Protection and adaptation policy approaches. Sci. Total Environ. 601–602, 441–452. https://doi.org/10.1016/j.scitotenv.2017.05.197.
Kowalzig, J., 2008. Climate, poverty, and justice: what the Poznan UN climate conference needs to deliver for a fair and effective global deal. Oxfam Policy Practice: Clim. Change Resilience 4 (3), 117–148.
Kundu, S., Khare, D., Mondal, A., 2017. Past, present and future land use changes and their impact on water balance. J. Environ. Manage. 197, 582–596. https://doi.org/10.1016/j.jenvman.2017.04.018.
Kushwaha, A., Jain, M.K., 2013. Hydrological simulation in a forest dominated watershed in Himalayan region using SWAT model. Water Resour. Manage. 27 (8), 3005–3023.
Lenhart, T., Eckhardt, K., Fohrer, N., Frede, H.-G., 2002. Comparison of two different approaches of sensitivity analysis. Phys. Chem. Earth 27 (9-10), 645–654.
Li, Y., Grimaldi, S., Pauwels, V.R.N., Walker, J.P., 2018. Hydrologic model calibration using remotely sensed soil moisture and discharge measurements: the impact on predictions at gauged and ungauged locations. J. Hydrol. 557, 897–909. https://doi.org/10.1016/j.jhydrol.2018.01.013.
Li, Y., Grimaldi, S., Walker, J., Pauwels, V.J.R.S., 2016. Application of remote sensing data to constrain operational rainfall-driven flood forecasting: a review. Remote Sens. 8 (6), 456.
Luber, G., Lemery, J., 2015. Global Climate Change and Human Health: From Science to Practice.
Maggioni, V., Massari, C., 2018. On the performance of satellite precipitation products in riverine flood modeling: a review. J. Hydrol. 558, 214–224.
McMichael, A.J., 2003. Climate Change and Human Health: Risks and Responses. World Health Organization.
Modarres, R., Sarhadi, A.J., 2009. Rainfall trends analysis of Iran in the last half of the twentieth century. J. Geophys. Res. Atmosph. 114 (D3).
Morgan, R.P.C., 2005. Soil Erosion and Conservation. Blackwell Publ., Oxford, UK.
Morris, J., Hess, T., Posthumus, H.J, 2010. Agriculture's Role in Flood Adaptation and Mitigation. OECD Studies on Water, pp. 1–35.
Napolitano, P., Fabbri, A., 1996. Single-parameter sensitivity analysis for aquifer vulnerability assessment using DRASTIC and SINTACS. IAHS Publications-Series of Proceedings and Reports-Intern Assoc. Hydrological Sciences, 235, pp. 559–566.
Napolitano, P., Fabbri, A.J., Sciences, R.-I.A.H., 1996. Single-parameter sensitivity analysis for aquifer vulnerability assessment using DRASTIC and SINTACS. IAHS Publications-Series of Proceedings and Reports-Intern Assoc Hydrological Sciences, 235, pp. 559–566.
Neale, T., Weir, J.K., 2015. Navigating scientific uncertainty in wildfire and flood risk mitigation: a qualitative review. Int. J. Disaster Risk Reduct. 13, 255–265. https://doi.org/10.1016/j.ijdrr.2015.06.010.
Nefeslioglu, H.A., Sezer, E.A., Gokceoglu, C., Ayas, Z., 2013. A modified analytical hierarchy process (M-AHP) approach for decision support systems in natural hazard assessments. Comput. Geosci. 59, 1–8.
Ni, J.R., Li, Y.K., 2003. Approach to soil erosion assessment in terms of land-use structure changes. J. Soil Water Conserv. 58 (3), 158–169.
NSWRI, 2016. National Soil and Water Research Institute of Iran Ministry of Agriculture http://www.swri.ir/.
O'Connell, P., Ewen, J., O'Donnell, G., Quinn, P.J.H., Sciences, E.S., 2007. Is there a link between agricultural land-use management and flooding? Hydrol. Earth Syst. Sci. 11 (1), 96–107.
Ouma, Y.O., Tateishi, R.J.W., 2014. Urban flood vulnerability and risk mapping using integrated multi-parametric AHP and GIS: methodological overview and case study assessment. Water 6 (6), 1515–1545.
Panagos, P., Meusburger, K., Alewell, C., Montanarella, L.J.E.M., 2012. Software Soil erodibility estimation using LUCAS point survey data of Europe. Environ. Modell. 30, 143–145.
Papaioannou, G., Vasiliades, L., Loukas, A.J., 2015. Multi-criteria analysis framework for potential flood prone areas mapping. Water Resour. Manage. 29 (2), 399–418.
Saaty, T.L., 1980. The Analytic Hierarchy Process: Planning. Priority Setting. Resource Allocation. International Book Company, MacGraw-Hill, New York, pp. 287.
Saaty, T.L., Vargas, L.G., 2001. Models, Methods, Concepts & Applications of the Analytic Hierarchy. Process–Kluwer Academic Publishers, Boston.
Salazar, S., et al., 2009. Efficiency of non-structural flood mitigation measures: "room for the river" and "retaining water in the landscape". Flood Risk Management: Research and Practice, pp. 723–731.
Sampson, C.C., et al., 2015. A high-resolution global flood hazard model. Water Resour. Res. 51 (9), 7358–7381.
Scrinzi, G., et al., 2006. Un modello di valutazione della funzionalità protettiva del bosco per la pianificazione forestale: la componente stabilità dei versanti rispetto ai fenomeni franosi superficiali. J. Silvic. Forest Ecol. 3 (1), 98.
Shi, P., et al., 2011. Evaluating the SWAT model for hydrological modeling in the Xixian watershed and a comparison with the XAJ model. Water Resour. Manage. 25 (10), 2595–2612.
Sinha, R., Bapalu, G., Singh, L., Rath, B., 2008. Flood risk analysis in the Kosi river basin, north Bihar using multi-parametric approach of analytical hierarchy process (AHP). J. Indian Soc. Remote Sens. 36 (4), 335–349.
Tabari, H., Abghari, H., Hosseinzadeh Talaee, P.J.H.P., 2012. Temporal trends and spatial characteristics of drought and rainfall in arid and semiarid regions of Iran. Hydrol. Process. 26 (22), 3351–3361.
Tehrany, M.S., Pradhan, B., Jebur, M.N., 2013. Spatial prediction of flood susceptible areas using rule based decision tree (DT) and a novel ensemble bivariate and multivariate statistical models in GIS. J. Hydrol. 504, 69–79.
Tehrany, M.S., Pradhan, B., Jebur, M.N., 2014a. Flood susceptibility mapping using a novel ensemble weights-of-evidence and support vector machine models in GIS. J. Hydrol. 512 (Supplement C), 332–343. https://doi.org/10.1016/j.jhydrol.2014.03.008.
Tehrany, M.S., Pradhan, B., Jebur, M.N., 2014b. Flood susceptibility mapping using a novel ensemble weights-of-evidence and support vector machine models in GIS. J. Hydrol. 512, 332–343.
Tehrany, M.S., Pradhan, B., Mansor, S., Ahmad, N., 2015. Flood susceptibility assessment using GIS-based support vector machine model with different kernel types. Catena 125, 91–101.
Thieken, A.H., Kreibich, H., Müller, M., Merz, B.J.H.S.J., 2007. Coping with floods: preparedness, response and recovery of flood-affected residents in Germany in 2002. Hydrol. Sci. J. 52 (5), 1016–1037.
Udin, W.S., Binti Ismail, N.A., Bahar, A.M.A., Khan, M.M.A., 2018. GIS-based River flood hazard mapping in rural area: a case study in Dabong, Kelantan, Peninsular Malaysia. Asian J. Water Environ. Pollut. 15 (1), 47–55.
Wang, Y., Li, Z., Tang, Z., Zeng, G., 2011. A GIS-based spatial multi-criteria approach for flood risk assessment in the Dongting Lake Region, Hunan, Central China. Water Resour. Manage. 25 (13), 3465–3484.
Woldesenbet, T.A., Elagib, N.A., Ribbe, L., Heinrich, J., 2018. Catchment response to climate and land use changes in the Upper Blue Nile sub-basins, Ethiopia. Sci. Total Environ. 644, 193–206. https://doi.org/10.1016/j.scitotenv.2018.06.198.
Wright, A.J., Walker, J.P., Pauwels, V.R.N., 2018. Identification of hydrologic models, optimized parameters, and rainfall inputs consistent with in situ streamflow and rainfall and remotely sensed soil moisture. J. Hydrometeorol. 19 (8), 1305–1320. https://doi.org/10.1175/jhm-d-17-0240.1.
Xiao, Y., Yi, S., Tang, Z., 2017. Integrated flood hazard assessment based on spatial ordered weighted averaging method considering spatial heterogeneity of risk preference. Sci. Total Environ. 599, 1034.
Zhao, G., Pang, B., Xu, Z., Yue, J., Tu, T., 2018. Mapping flood susceptibility in mountainous areas on a national scale in China. Sci. Total Environ. 615 (Supplement C), 1133–1142. https://doi.org/10.1016/j.scitotenv.2017.10.037.